Materials Today: Proceedings xxx (xxxx) xxx

Contents lists available at ScienceDirect

Materials Today: Proceedings

journal homepage: www.elsevier.com/locate/matpr

Structural and optical investigations of biosynthesized bunsenite NiO nanoparticles (NPs) via an aqueous extract of *Rosmarinus officinalis* (rosemary) leaves

S.K. Noukelag [b,c,*], H.E.A. Mohamed [a,b], B. Moussa [a,b], L.C. Razanamahandry [d], S.K.O. Ntwampe [e,f], C.J. Arendse [c]

[a] *UNESCO-UNISA Africa Chair in Nanosciences-Nanotechnology Laboratories (U2AC2N), College of Graduate Studies, University of South Africa (UNISA), Muckleneuk Ridge, PO Box 392, Pretoria, South Africa*
[b] *Nanosciences African Network (NANOAFNET), Material Research Department (MRD), iThemba LABS-National Research Foundation, 1 Old Faure Road, Somerset West 7129, PO Box 722, Somerset West, Western Cape, South Africa*
[c] *Department of Physics and Astronomy, University of the Western Cape, Robert Sobukwe Road, Private Bag X17, Bellville 7535, South Africa*
[d] *African Union Development Agency, Economic Integration Division, PO Box 1685, Johannesburg, South Africa*
[e] *Bioresource Engineering Research Group (BioERG), Cape Peninsula University of Technology, PO Box 652, Cape Town, 8000, South Africa*
[f] *School of Chemical and Minerals Engineering, North West University, Potchefstroom Campus Private Bag X6001, Potchefstroom 2520, South Africa*

A R T I C L E I N F O

Article history:
Received 16 August 2019
Received in revised form 9 March 2020
Accepted 13 March 2020
Available online xxxx

Keywords:
Green synthesis
NiO
Nanoparticles
Rosmarinus officinalis (rosemary)
Extract
Electron microscopy

A B S T R A C T

Green synthesis of nanoparticles represents an important part of nanotechnology that offers outstanding eco-friendly and financial benefits when compared to conventional methods that use toxic substances and involve complex processes. In this paper, we report a completely green process in which aqueous extract of rosemary leaves containing bioactive molecular compounds (flavonoids, monoterpenoids, phenolic acids, and diterpenoids) acted as both chelating and stabilizing agents to facilitate the synthesis of NiO NPs. Apart from the nickel metal precursor, the synthesis was free of solvents and surfactants in this method to adhere to green chemistry principles and the impartation of environmental benignity. To achieve the aim of the study, structural and optical property analyses of Bunsenite annealed at 500 °C were carried-out using complementary techniques namely high resolution transmission electron microscopy (HRTEM), selected area electron diffraction (SAED), X-ray diffraction (XRD), energy dispersive X-ray spectroscopy (EDS), attenuated total reflection-Fourier transform infrared spectroscopy (ATR-FTIR) and UV–Vis-NIR absorption spectroscopy. HRTEM micrographs revealed the self-assembled, highly agglomerated quasi-spherical shaped NPs with a cubic structure and the average size was found to peak at 8.09 ± 0.20 nm. SAED and XRD exhibited the polycrystallinity and the purity of NiO NPs and the average size was found in the range of 11.598–15.527 nm. Besides, EDS depicted the presence of Ni and O in the sample while ATR-FTIR illustrated the Ni-O chemical bonds. From UV–Vis-NIR, the optical band gap amounted to 3.39 eV confirmed the formation of NiO NPs. Thereby, an easy and effective green approach for the synthesis of Bunsenite with efficient properties is reported.

Selection and peer-review under responsibility of the scientific committee of the NANOSMATAFRICA-2018.

1. Introduction

Nanoparticles are collections of atoms bonded together in smallest sizes in the nano-range with highly attractive property in their large surface area which makes it more efficient to interact with other molecules when added to suspensions [1,2]. Metallic oxide nanoparticles, specifically nano-scale NiO has attracted considerable attention in recent decades due to its high chemical stability, electrocatalysis, electron transfer capabilities, and supercapacitance properties. Bunsenite is an environmentally friendly material, a p-type semiconductor metal oxide with a wide bandgap ranging from 3.6 to 4.0 eV [3,4]. In terms of synthesis, several chemical and physical methods are commonly used. Chemical synthesis routes often generate toxic chemical waste and residue while physical synthesis methods are energy-intensive [5–7].

* Corresponding author.
E-mail address: sandrinedoum@yahoo.fr (S.K. Noukelag).

https://doi.org/10.1016/j.matpr.2020.03.314
2214-7853/
Selection and peer-review under responsibility of the scientific committee of the NANOSMATAFRICA-2018.

Please cite this article as: S. K. Noukelag, H. E. A. Mohamed, B. Moussa et al., Structural and optical investigations of biosynthesized bunsenite NiO nanoparticles (NPs) via an aqueous extract of *Rosmarinus officinalis* (rosemary) leaves, Materials Today: Proceedings, https://doi.org/10.1016/j.matpr.2020.03.314

Consequently, an alternative and environmentally benign synthesis route that adheres to the green chemistry approach involving phytoexudes or extracts is becoming a popular approach for nanoparticles synthesis and advocated for its rapidity, simplicity, minimized energy intensity thus reduced synthesis costs with minimum waste generation to produce the desired metal oxides NPs [8–10]. Plant extracts such as those from *Callistemon viminalis* (Weeping bottlebrush) *Sageretia thea* (Osbeck), *Aspalathus linearis* (Rooibos), *Agathosma betulina* (Buchu), *Aegle marmelos* L. (Bael) have been used as capping, reducing, chelating, and stabilizing agents for NiO nanoparticles [4,11–14] except leaves extract from *Rosmarinus officinalis*, commonly known as rosemary has not been reported in the literature as a viable source for the synthesis of Bunsenite to the best of our knowledge.

Rosemary is a drought-tolerant wild shrub that grows up to two meters high, with small green leaves. Although it is a native plant of the Mediterranean region, it can be cultivated around the world due to its hardiness albeit this is variety dependent. Current uses include its use as a natural food preservative and flavoring agent. Besides, it is also a valuable and important medicinal and aromatic plant [15–18]. Major constituents of rosemary leaves extract are listed in Table 1 and their structure in Fig. 1.

In this contribution, we report on the novel green synthesis of NiO nanoparticles from *Rosmarinus officinalis* (rosemary) leaves extract. The morphology, the crystallinity, the structure, the vibrational and the optical properties of Bunsenite are presented, a study reported herein for the first time.

2. Material and methods

2.1. Biosynthesis

Rosemary leaves were purchased from Western Cape Province-South Africa. Nickel nitrate hexahydrate $Ni(NO_3)_2{\cdot}6H_2O$ was purchased as an analytical grade reagent (Sigma Aldrich, Modderfontein, South Africa). 10 g of rosemary leaves were weighed and washed with sterile distilled water at ambient temperature.

Subsequently, they were immersed in 200 mL of deionized water to extract phytoexudes, a process achieved by boiling at 80 °C for 2 h. The resultant extracts' pH was found to be 5.7. The extract solution was filtered twice to eliminate residual solids after the addition of 6 g/100 mL extracts of the precursor salt, i.e. nickel nitrate, which was homogeneously mixed at 60 °C for 1 h. Thereafter, a slight acidification of the resultant solution was observed, with a final pH of 4.8. It was cooled down to ambient temperature and kept in a drying oven at 100 °C. The dried powder was annealed in a ceramic crucible at 500 °C in an open-air furnace for 2h leading to nanoparticles of a highly crystalline character that changed color from greyish-brown precipitate to black.

Table 1
The major chemical composition of rosemary leaves extract.

Flavonoids	Pelargonidin-3,5-diglucoside (I)
	Cyanidin-3,5-diglucoside (II)
	Kaempherol (III)
Monoterpenoids	α -pinene (IV)
	1,8-cineole
	Camphor
Phenolic acids	Rosmarinic
	Caffein acid
Diterpenoids	Carnosol
	Methyl carnosate
	12-methoxycarnosic acid
	Epi- and iso-rosmanol

2.2. Characterizations

Various techniques were used to characterize and investigate structural and optical properties Bunsenite annealed at 500 °C.

HRTEM using a Joel JEM 4000EX electron microscopy unit with a resolution limit of about 0.12 nm at an accelerating voltage of 200 kV combined to SAED was used to study morphology, shape, and the crystallinity; X-ray diffractometer (model Bruker AXS D8 Advance) with irradiation line Kα1 of copper (λCuKα1 = 1.5406 Å) operating at a voltage of 40 kV and a current of 35 mA, in the angular range of 20-90° was used to study the crystalline nature and the structure; Similarly, EDS analysis was executed to determine elemental composition whereby an EDS Oxford instrument X-Max solid-state silicon drift detector operating at 20 kV was used. ATR-FTIR absorption spectrometer (Thermo Nicolet 8700 FTIR spectrometer) was used in the spectral range 400–4000 cm^{-1} to ascertain the surface coating and chemical bonding. Finally, UV–VIS-NIR experiment was conducted using a Nicolette Evolution 100 Spectrophotometer to analyze the optical properties in the spectral range 200–800 nm.

3. Results & discussions

3.1. Morphology and microscopy observations

The morphology, the shape and the crystallinity of Bunsenite annealed at 500 °C for 2 h were investigated by HRTEM and SAED as presented in Fig. 2. One can notice that the NPs are highly agglomerated and quasi-spherical shaped. By fitting the histogram data with a Gaussian distribution, the average size was found to peak at 8.09 ± 0.20 nm. The SAED exhibits several diffraction rings with strong diffraction spots. The bulk of nanoparticles appeared to be polycrystalline. From these results, it was established that the Bunsenite is generally cubically structured [4,12,14].

3.2. Crystallographic analysis

The crystal structure of NiO NPs annealed at 500 °C for 2 h was confirmed by XRD as presented in Fig. 3. Five sharp and strong Bragg peaks were observed with their maxima centered at 2θ ~ 37.249°, 43.276°, 62.879°, 75.416°, and 79.409° may be indexed to cubic NiO known also as the "Bunsenite" phase which agreed with the data of the Joint Committee on Powder Diffraction Standards (JCPDS file No.047–1049). The Bragg peaks are ascribed to crystallographic reflection correspond to (1 1 1), (2 0 0), (2 2 0), (3 1 1) and (2 2 2) crystal planes. The strong sharp diffraction peaks demonstrated highly crystalline NiO NPs. The crystallite size was calculated from peak broadening analysis, i.e. diffraction peaks, using Debye-Scherrer formula $\langle øparticles\rangle \sim 0.9\lambda/(\Delta\theta 1/2 \cos\theta B)$. In this equation, λ represents the wavelength of X-ray radiation (1.5406), Δθ1/2 the full width and half maximum of the diffraction peak and θB the Bragg's angle. The average size of annealed NiO NPs was found in the range of 11.598 to 15.527 nm. The deduced lattice constant *a* calculated using the relationship $1/dhkl = (1/a)((h^2 + k^2 + l^2)^{1/2})$ is $\langle a\rangle = 4.177$ Å whereby *h*, *k*, *l* are the miller indices.

The XRD pattern confirmed the formation of a pure face centered cubic NiO NPs. We notice that the size obtained from XRD analysis, are slightly higher than the size obtained from TEM micrographs [19,20].

Table 2 illustrates the major XRD characteristics of the various Bragg diffraction peaks of Bunsenite.

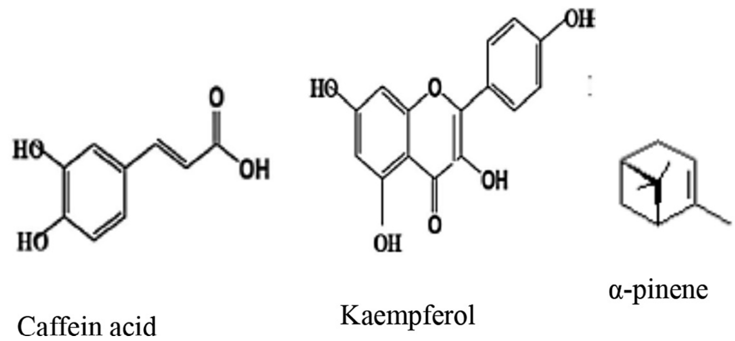

Fig. 1. Structure of major bioactive molecular compounds in rosemary leaves extract.

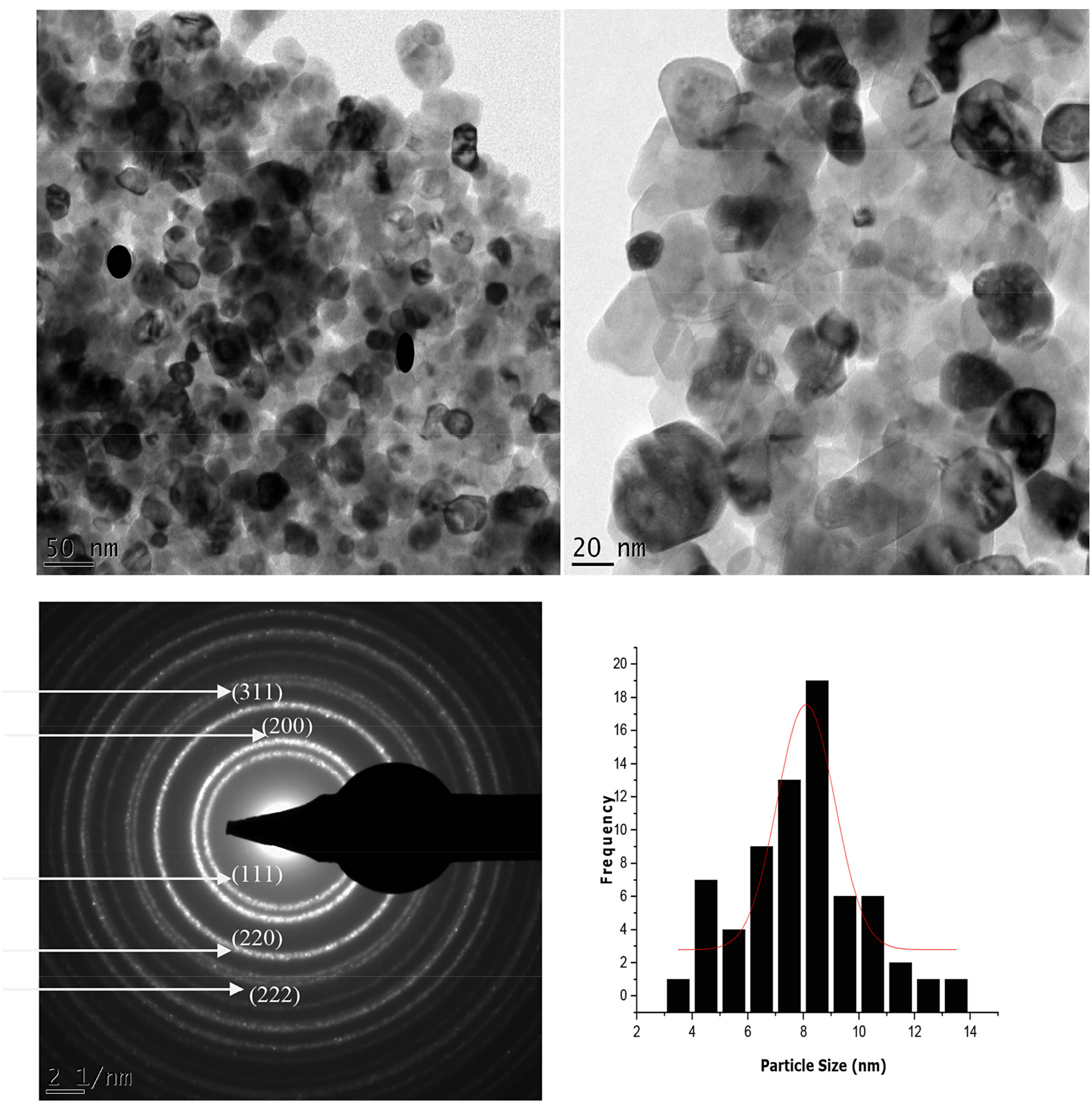

Fig. 2. HRTEM micrographs combined with SAED and the average size distribution of NiO NPs annealed at 500 °C for 2 h.

Please cite this article as: S. K. Noukelag, H. E. A. Mohamed, B. Moussa et al., Structural and optical investigations of biosynthesized bunsenite NiO nanoparticles (NPs) via an aqueous extract of *Rosmarinus officinalis* (rosemary) leaves, Materials Today: Proceedings, https://doi.org/10.1016/j.matpr.2020.03.314

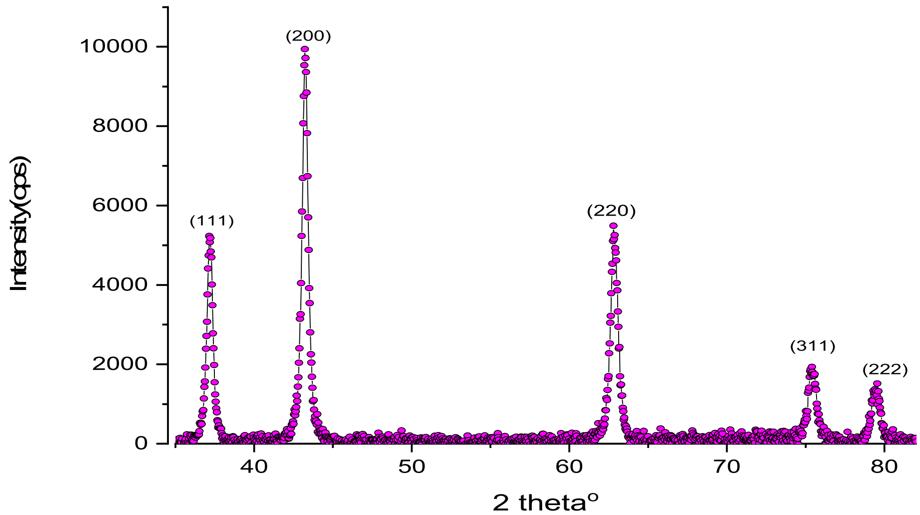

Fig. 3. XRD pattern of crystalline NiO NPs annealed at 500 °C for 2 h.

Table 2
The major X-ray diffraction (XRD) characteristics of the various Bragg diffraction peaks.

Material	Miller Indices	2θ degrees	Θ (Radians)	FWHM (radians)	Average size<Φ>(nm)	<dhkl>(nm)
NiO	(1 1 1)	37.249	0.325	0.0105	15.527	2.411
NiO	(2 0 0)	43.276	0.377	0.0143	11.598	2.088
NiO	(2 2 0)	62.879	0.548	0.0141	12.897	1.476
NiO	(3 1 1)	75.416	0.658	0.0143	13.623	1.259
NiO	(2 2 2)	79.409	0.693	0.0140	14.303	1.205

3.3. Elemental analysis

For elemental composition by EDS, the obtained profile of annealed NiO nanoparticles at 500 °C for 2 h is shown in Fig. 4. The presence of nickel and oxygen atoms is confirmed. The peak due to carbon emanates from the carbon tape used to immobilize NiO NPs and to minimize charging effects. The peaks due to K, Cl, N, and Na were hypothesized to emanate from the rosemary leaves extract. Further FTIR analysis is done to confirm their purity.

3.4. Vibrational and optical properties

To detect any additional surface/interface bound compounds, functional groups and the validation of NiO NPs annealed at 500 °C for 2h, ATR-FTIR was carried out with different absorption bands as showed in Fig. 5.

The vibration modes observed at 569 cm^{-1} is associated with a typical metal oxide with single bonds in the bending mode. So, the strong absorption bands at 569 cm^{-1}, 924 and 1031 cm^{-1} were attributed to the Ni-O bonds in the bending mode. The absorption band 1387 cm^{-1} was assigned the C = O, CH_3 and C = C aromatic functional groups associated with various bioactive compounds in the Rosemary leaves extracts. The weak bands at 1645 and 3468 cm^{-1} may well be attributed to moisture absorbed/adsorbed on to the surface of the nanoparticles and the (OH) hydroxyl groups, respectively [4,11,13].

The reflectance of NiO nanoparticles annealed at 500 °C for 2 h is reported in Fig. 6. The peak at 365 nm in the absorption spectrum

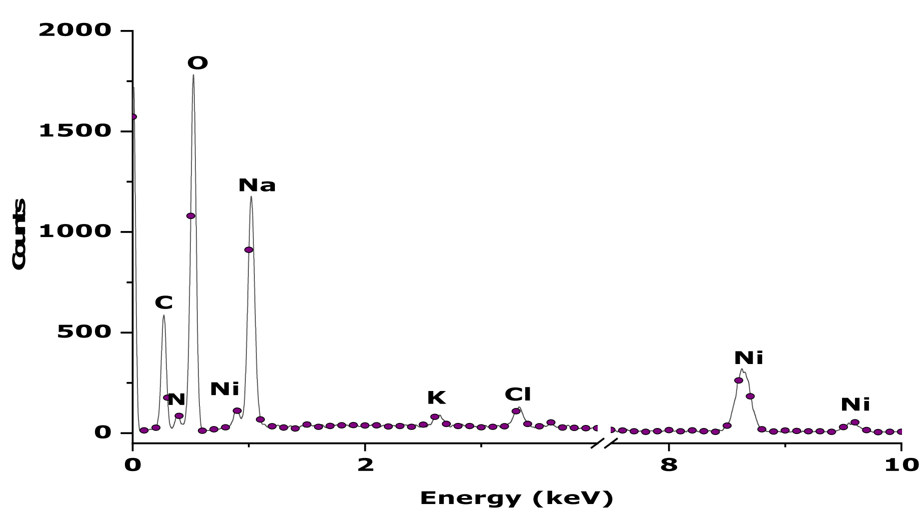

Fig. 4. EDS spectrum of NiO NPs annealed at 500 °C for 2 h.

Please cite this article as: S. K. Noukelag, H. E. A. Mohamed, B. Moussa et al., Structural and optical investigations of biosynthesized bunsenite NiO nanoparticles (NPs) via an aqueous extract of *Rosmarinus officinalis* (rosemary) leaves, Materials Today: Proceedings, https://doi.org/10.1016/j.matpr.2020.03.314

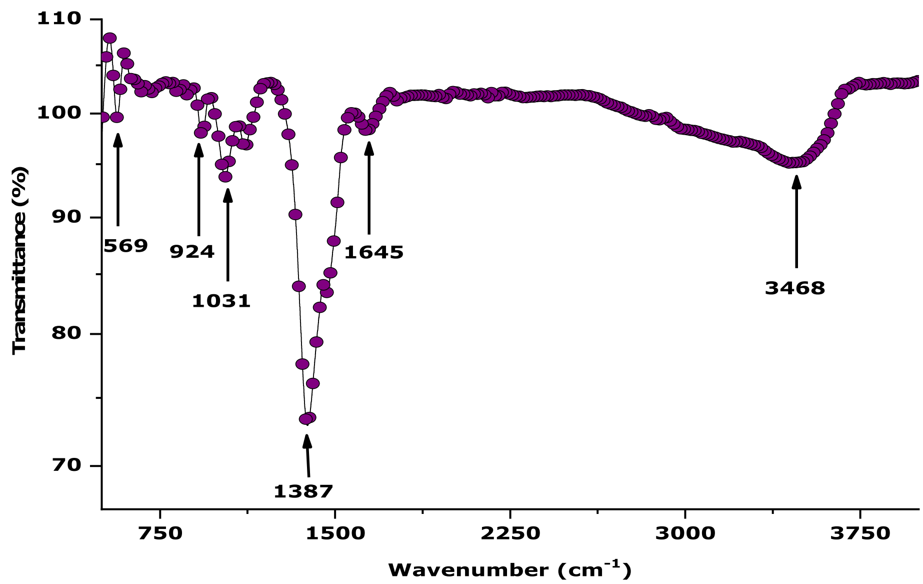

Fig. 5. ATR-FTIR spectrum of NiO NPs annealed at 500 °C for 2 h.

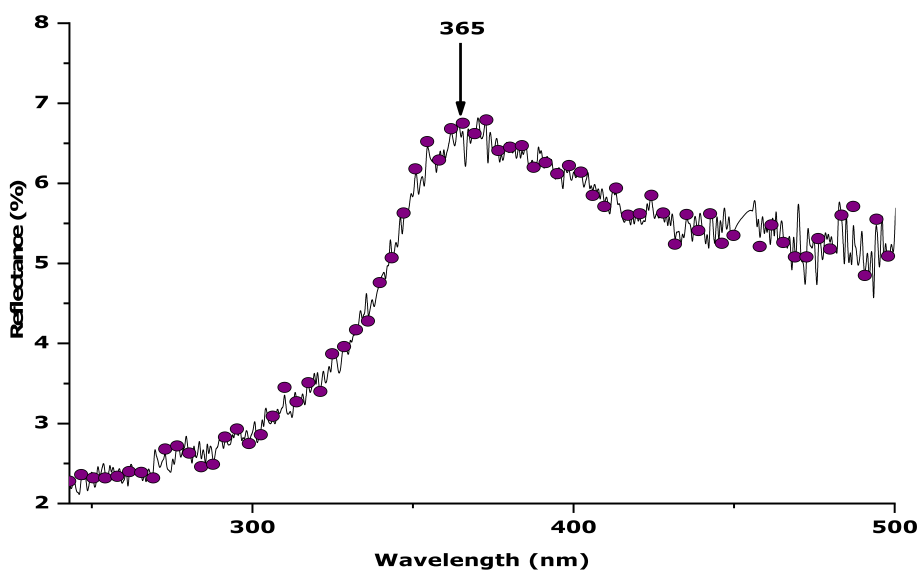

Fig. 6. UV–Vis spectrum of NiO NPs annealed at 500 °C for 2 h.

confirmed the formation of NiO NPs and is associated with a charge transfer from the band of conduction to the band of valence cations [10,14]. Direct bandgap was computed using the formula Eg = 1240/λ and was amounted to 3.39 eV whereby Eg is the optical band gap, with 1240 being the value of the photon energy while λ is the wavelength.

4. Conclusion

Bunsenite NiO nanoparticles was successfully synthesized by reduction of $Ni(NO_3)_2{\cdot}6H_2O$ to NiO using an aqueous extract of rosemary leaves. The XRD pattern exhibited a Bunsenite structure with no secondary phases confirmed the formation of highly pure NiO nanoparticles with an average size ranging from 11.598 to 15.527 nm. HRTEM denoted highly agglomerated quasi-spherical shaped NiO nanoparticles while SAED confirmed their polycrystalline nature and the average size was found to peak at 8.09 ± 0.20 nm. Besides that, EDS and ATR-FTIR elucidated the presence of Ni and O in the sample. Finally, from UV–Vis, the energy bandgap amounted to 3.39 eV confirmed the formation of NiO NPs. This green synthesis pathway demonstrated the importance of rosemary leaves extract as cost-effective, cheap and environmental benignity to facilitate the synthesis of Bunsenite NiO nanoparticles.

CRediT authorship contribution statement

S.K. Noukelag: Conceptualization, Visualization, Investigation Methodology, Data curation, Writing - original draft, Writing - review & editing. **H.E.A. Mohamed:** Writing - review & editing. **B. Moussa:** Writing - review & editing. **L.C. Razanamahandry:** Writing - review & editing. **S.K.O. Ntwampe:** Writing - review & editing. **C.J. Arendse:** Supervision.

Please cite this article as: S. K. Noukelag, H. E. A. Mohamed, B. Moussa et al., Structural and optical investigations of biosynthesized bunsenite NiO nanoparticles (NPs) via an aqueous extract of *Rosmarinus officinalis* (rosemary) leaves, Materials Today: Proceedings, https://doi.org/10.1016/j.matpr.2020.03.314

Declaration of Competing Interest

The authors declare that they have no known competing financial interests or personal relationships that could have appeared to influence the work reported in this paper.

Acknowledgments

This research program was generously supported by grants from the National Research Foundation of South Africa (NRF) (NRF MM 4200220), the UNESCO-UNISA Africa Chair in Nanosciences & Nanotechnology (UNESCO-UNISA MM 4200220), iThemba LABS, the Academy of Sciences for the Developing World (TWAS) (TWAS MM 4200220), the University of the Western Cape (UWC) as well as Cape Peninsula University of Technology (CPUT) to whom we are all grateful.

References

[1] L. Vayssieres, On the design of advanced metal oxide nanomaterials, Int. J. Nanotechnol., vol. 1, no. 1, pp. 1–41, 2004.
[2] M. Fernández-Garcia, J. Rodriguez, Metal Oxide Nanoparticles. Manuscript submitted for publishing, Nanomaterials: Inorganic and Bioinorganic Perspectives, 2007.
[3] N. Mayedwa, N. Mongwaketsi, S. Khamlich, K. Kaviyarasu, N. Matinise, M. Maaza, Green synthesis of nickel oxide, palladium and palladium oxide synthesized via aspalathus linearis natural extracts: physical properties and mechanism of formation, Appl. Surface Sci., doi: 10.1016/j.apsusc.2017.12.116.
[4] A.K.H. Bashir, L.C. Razanamahandry, A.C. Nwanya, K. Kaviyarasu, W. Saban, H.E. A. Mohamed, S.K.O. Ntwampe, F.I. Ezema, M. Maaza, Biosynthesis of NiO nanoparticles for photodegradation of free cyanide solutions under ultraviolet light, J. Phys. Chem. Solids 134 (2019) 133–140.
[5] K. Anandan, V. Rajendran, Morphological and size effects of NiO nanoparticles via solvothermal process and their optical properties, Mater. Sci. Semicond. Process 14 (2011) (43).
[6] K. Anandan, V. Rajendran, Structural, optical and magnetic properties of well dispersed NiO nanoparticles synthesized by CTAB assisted solvothermal process, Int. J. Nanosci. Nanotechnol. 2 (4) (2012) 24–29.
[7] A.K. Ramasami, M.V. Reddy, G.R. Balakrishna, Combustion synthesis and characterization of NiO nanoparticles, Mater. Sci. Semicond. Process 40 (2015) 194–202.
[8] B.E.V. Wyk, B.V. Oudtshoorn, N. Gericke, Medicinal Plants of South Africa, Briza Publication, Pretoria, South Africa, 2013.
[9] S. Baker, D. Rakshith, K.S. Kavitha, P. Santosh, H.U. Kavitha, Y. Rao, S.S. Satish, Plants: emerging as nanofactories towards facile route in synthesis of nanoparticles, BioImpacts 3 (2013) 111–117.
[10] A.C. Nwanya, M.M. Ndipingwi, C.O. Ikpo, R.M. Obodo, S.C. Nwanya, S. Botha, F.I. Ezema, E.I. Iwuoha, M. Maaza, Zea mays lea silk extract mediated synthesis of nickel oxide nanoparticles as positive electrode material for asymmetric supercabattery, J. Alloys Compounds 822 (2020) 153581.
[11] B.T. Sone, X.G. Fuku, M. Maaza, Physical & electrochemical properties of green synthesized bunsenite NiO nanoparticles via Callistemon viminalis' extracts, Int. J. Electrochem. Sci. 11 (2016) 8204–8220.
[12] A.T. Khalil, M. Ovais, I. Ullah, M. Ali, Z.K. Shinwari, D. Hassan, M. Maaza, Sageretia thea (Osbeck.) modulated biosynthesis of NiO nanoparticles and their in vitro pharmacognostic, antioxidant and cytotoxic potential, Artificial Cells, Nanomed. Biotechnol. (2017).
[13] F.T. Thema, E. Manikandan, A. Gurib-Fakim, M. Maaza, Single phase Bunsenite NiO nanoparticles green synthesis by Agathosma betulina natural extract, J. Alloys Compounds 657 (2016) 655–661.
[14] A.A. Ezhilarasi, J.J. Vijaya, K. Kaviyarasu, L.J. Kennedy, R. Jothiramalingam, H.A. Al-Lohedan, Green synthesis of NiO nanoparticles using Aegle marmelos leaf extract for the evaluation of in-vitro cytotoxicity, antibacterial and photocatalytic properties. doi: 10.1016/j.jphotobiol.2018.01.023.
[15] V. Queralt, R.J. Anna, M. Huélamo, Miriam, R. Alvarenga, J. Fernando, Leal, L. Neto, L. Raventos, M. Rosa, A comprehensive study on the phenolic profile of widely used culinary herbs and spices: rosemary, thyme, oregano, cinnamon, cumin and bay. Food Chem., 154: 29907. doi: 10.1016/j.foodchem.2013.12.106. PMID 24518346.
[16] J. Rafael de Oliveira, S.E.A. Camargo, L. Dias de Oliveira, Rosmarinus officinalis L. (rosemary) as therapeutic and prophylactic agent, J. Biomed. Sci. (2019), https://doi.org/10.1186/s12929-019-0499-8.
[17] M.R. Al-Sereitia, K.M. Abu-Amerb, P. Sena, Pharmacology of rosemary (Rosmarinus officinalis Linn.) and its therapeutic potentials. Indian J. Exp. Biol. 37, 124–131, 1999.
[18] P.G. Peiretti, G. Francesco, O. Marco, R. Aigotti, C. Medana, Effects of rosemary oil (*Rosmarinus officinalis*) on the shelf-life of minced rainbow trout (*Oncorhynchus mykiss*) during refrigerated storage, Foods 1 (2012) 28–39, https://doi.org/10.3390/foods1010028.
[19] K.M. Srivastava, S.A. Ojha, K. Chaubey, C.P. Sharma, A. Pandey, J. Alloys Comp. 494 (2010) 275–284.
[20] K.M. Srivastava, S.A. Ojha, S. Chaubey, J. Singh, J. Solid State Chem. 183 (2010) 2669–2674.